

10,04

Phonon spectrum of  $\text{La}_2\text{Ge}_2\text{O}_7$ : *ab initio* calculation

© V.A. Chernyshev, V.P. Petrov

Ural Federal University after the first President of Russia B.N. Yeltsin,  
Yekaterinburg, Russia

E-mail: vladimir.chernyshev@urfu.ru

Received April 22, 2022

Revised April 22, 2022

Accepted April 28, 2022

Within the framework of the density functional theory *ab initio* calculation of the crystal structure, phonon spectrum, and elastic properties of lanthanum germanate  $\text{La}_2\text{Ge}_2\text{O}_7$  with a triclinic structure (sp. gr.  $P\bar{1}$ , no. 2) was carried out. The frequencies and types of fundamental modes are determined. From the analysis of the displacement vectors obtained from the calculation, the degree of participation of ions in each mode was determined. The calculations were performed for the first time. Experimental data on the IR and Raman spectra, as well as the elastic constants of  $\text{La}_2\text{Ge}_2\text{O}_7$ , are absent in the scientific press. We used the CRYSTAL17 program designed for *ab initio* calculations of periodic structures within the framework of the MO LCAO approach.

**Keywords:** rare-earth germanates, phonons, elastic constants, hybrid functionals.

DOI: 10.21883/PSS.2022.08.54628.301

## 1. Introduction

Crystals  $R_2\text{Ge}_2\text{O}_7$ , where  $R$  — rare-earth ion, attract attention of researchers by variety of properties [1–5]. They are crystallized in various structural types [1,6]. According to X-ray diffraction analysis results,  $\text{La}_2\text{Ge}_2\text{O}_7$  has low symmetry triclinic structure [6,7] (Fig. 1), space group  $P\bar{1}$ ,  $Z = 4$ .

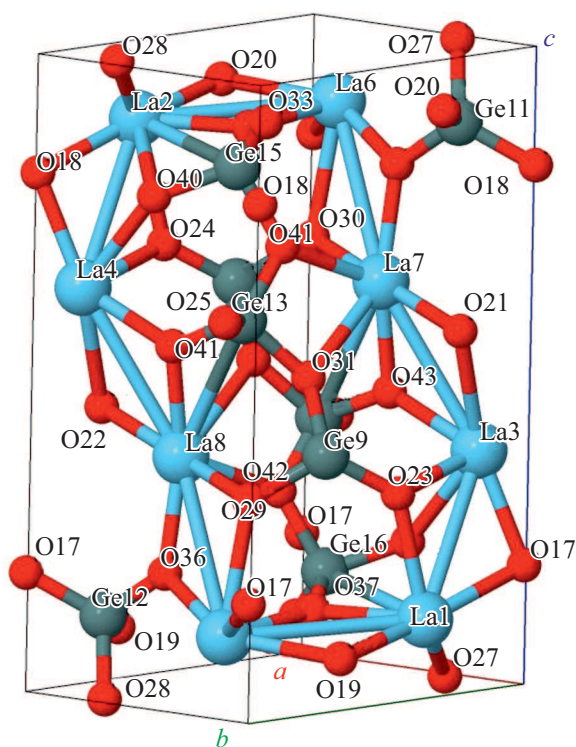


**Figure 1.** Crystalline structure  $\text{La}_2\text{Ge}_2\text{O}_7$  (sp. gr.  $P\bar{1}$ ,  $Z = 4$ ).

In paper [8] theoretical research of  $\text{La}_2\text{Ge}_2\text{O}_7$  was carried out in high symmetry pyrochlore structure (cubic syngony, sp. gr. 227). However, the corresponding experimental data is not available. Let us note that Materials Project website [9,10] also provides calculation results *ab initio* for  $\text{La}_2\text{Ge}_2\text{O}_7$  in triclinic syngony. The calculation was done for space groups  $P1$  [9] and  $P\bar{1}$  [10]. Calculation results in space group  $P\bar{1}$  [10] comply with experimental data [6,7]. Calculation in [10] was performed with functionality of GGA level, which made it possible to well reproduce crystalline structure, produced from X-ray diffraction analysis [7]. However, scientific publications lack information about elastic constants for  $\text{La}_2\text{Ge}_2\text{O}_7$ , both experimental and theoretical. There is no information on phonon spectrum for  $\text{La}_2\text{Ge}_2\text{O}_7$ . To calculate elastic constants and phonon spectrum for  $\text{La}_2\text{Ge}_2\text{O}_7$ , it seems relevant to use hybrid functionality, taking into account not only contributions of GGA level, but also contribution of non-local exchange in Hartree–Fock formalism.

In this paper we performed calculation *ab initio* for structure and properties of  $\text{La}_2\text{Ge}_2\text{O}_7$  both in low symmetry monoclinic structure (sp. gr.  $P\bar{1}$ ,  $Z = 4$ ), and in pyrochlore structure within the theory of density functionality with hybrid functionality PBE0.

## 2. Calculation methods

Calculations were made within theory of density functionality and approach of MO LCAO. Structure and properties of  $\text{La}_2\text{Ge}_2\text{O}_7$  both in low symmetry space group and in high symmetry structure of pyrochlore were calculated with hybrid functionality PBE0 [11], taking into account contribution of non-local exchange (in Hartree–Fock formalism), and also non-dynamic correlations [12]. Besides,

crystalline structure of  $\text{La}_2\text{Ge}_2\text{O}_7$  in both space groups was calculated with several functionalities of different level: non-hybrid PBE, hybrid B3LYP (20% XF-exchange) and PBE0 (25% XF exchange).

For calculations, CRYSTAL17 software was used, which is designed to model periodical structures.

To describe Ge and O, full electron basis sets [13,14] were used. To describe inner La shells, quasirelativistic pseudopotential ECP46MWB was used. To describe outer shells ( $5s^25p^6$ ), participating in formation of a chemical bond, a valent basis set of TZVP-type was used with diffuse and polarization  $s$ -,  $p$ - and  $d$ -orbitals ECP46MWB-I. Pseudopotential and valent basis set are available on website Stuttgart [15]. Integration by Brillouin zone was carried out using Monkhorst–Pack arrangement with mesh of  $k$ -dots  $8 \times 8 \times 8$ . Accuracy of two-electron integral calculation was  $10^{-8}$  Hartree min. When solving a system of one-electron Kohn–Sham equations, the accuracy of self-consistent field calculation was set as  $10^{-9}$  a.u. The following parameters of crystalline structure optimization were set. Mean square value of energy gradient was set as equal to 0.00030 a.u., maximum value of component — equal to 0.00045 a.u. Besides, during structure optimization, CRYSTAL software evaluates values of shear relative to the previous step: by mean square value and absolute value of the largest component. They were set as equal to 0.0012 and 0.0018 a.u. Optimization was deemed complete, if all four conditions were met simultaneously.

### 3. Discussion of the results

The calculation predicts that energy per one formula unit for  $\text{La}_2\text{Ge}_2\text{O}_7$ , will be lower in crystallization of low symmetry structure compared to that in pyrochlore structure. Table 1 shows the difference between pyrochlore structure energy and low symmetry structure energy (per one formula unit).

Calculations predict that low symmetry structure is energetically more advantageous. Besides, account of non-local exchange contribution in Hartree–Fock formalism (functionalities B3LYP and PBE0, Table 1) just enhance this advantage. This result is well agreed with PCA-experiment [7], where low symmetry structure  $\text{La}_2\text{Ge}_2\text{O}_7$  was observed.

Table 2 shows calculated (with PBE0 functionality) constant meshes and corners of elementary cell in low symmetry structure  $\text{La}_2\text{Ge}_2\text{O}_7$ .

**Table 1.** Difference between energy of pyrochlore structure and low symmetry structure ( $\Delta E = E_{\text{pyro}} - E_{\text{low symm}}$ ), per one formula unit

DFT functionality	$\Delta E$ , a.u.
PBE	0.045
PBE0 (25% XF)	0.053
B3LYP (20% XF)	0.069

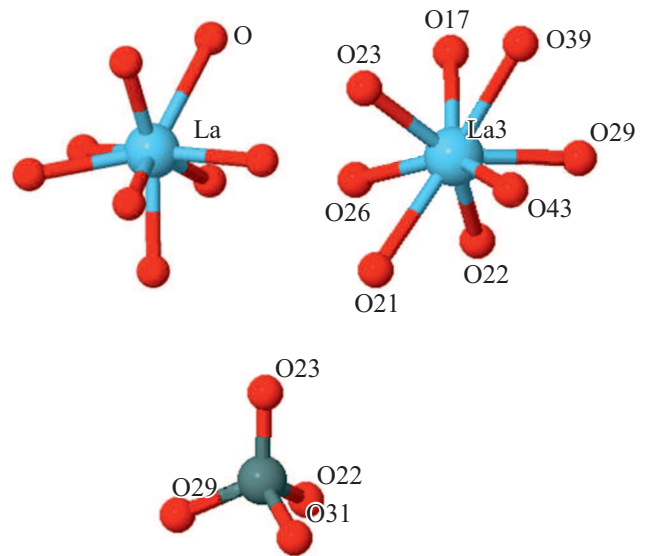


**Figure 2.** Local surrounding of La and Ge ions in low symmetry structure  $\text{La}_2\text{Ge}_2\text{O}_7$ .

Agreement with experiment [7] is good.

Ion coordinates in elementary cell are given in Table 3.

In pyrochlore structure, space group  $Fd\bar{3}m$  (no. 227), ions are in positions: Ge —  $16c$  (0, 0, 0), La —  $16d$  (1/2, 1/2, 1/2), O1 —  $48f$  ( $x$ , 1/8, 1/8), O2 —  $8b$  (3/8, 3/8, 3/8). Oxygen is in two symmetrically non-equivalent positions. Calculation with PBE0 functionality for such structure gives constant of mesh 10.331 Å and  $x = 0.32035$ .

In low symmetry structure rare-earth ion is surrounded by 8 oxygen ions. Ion Ge — surrounded by 4 oxygen ions (Fig. 2).

Charges of ions and charges on bonds (by Mulliken) for low symmetry structure are given in Table 4–5.

Calculation predicts substantial deviation of ion charges from their charges in the ion bond assumption. Calculation predicts minor charge on bond La–O, and substantial charge on bond Ge–O (Table 5).

It may be noted that in low symmetry structure of distances Ge–O is less than in pyrochlore structure. For pyrochlore structure the calculation predicts distance Ge–O, equal to 1.965 Å, while in low symmetry structure distances Ge–O are from 1.733 to 1.813 Å. Distances La–O are slightly less in pyrochlore structure, compared to low symmetry structure. In pyrochlore structure there are two oxygen ions at distance 2.237 Å and six oxygen ions at distance 2.604 Å from ion La. In low symmetry structure lanthanum is also surrounded by 8 oxygen ions, distances to which vary from 2.405 to 2.831 Å. It can be assumed that crystal field on La ion in low symmetry structure will be weaker than in pyrochlore structure.

The results of band structure calculation are shown in Figs. 3–4 and in Table 6.

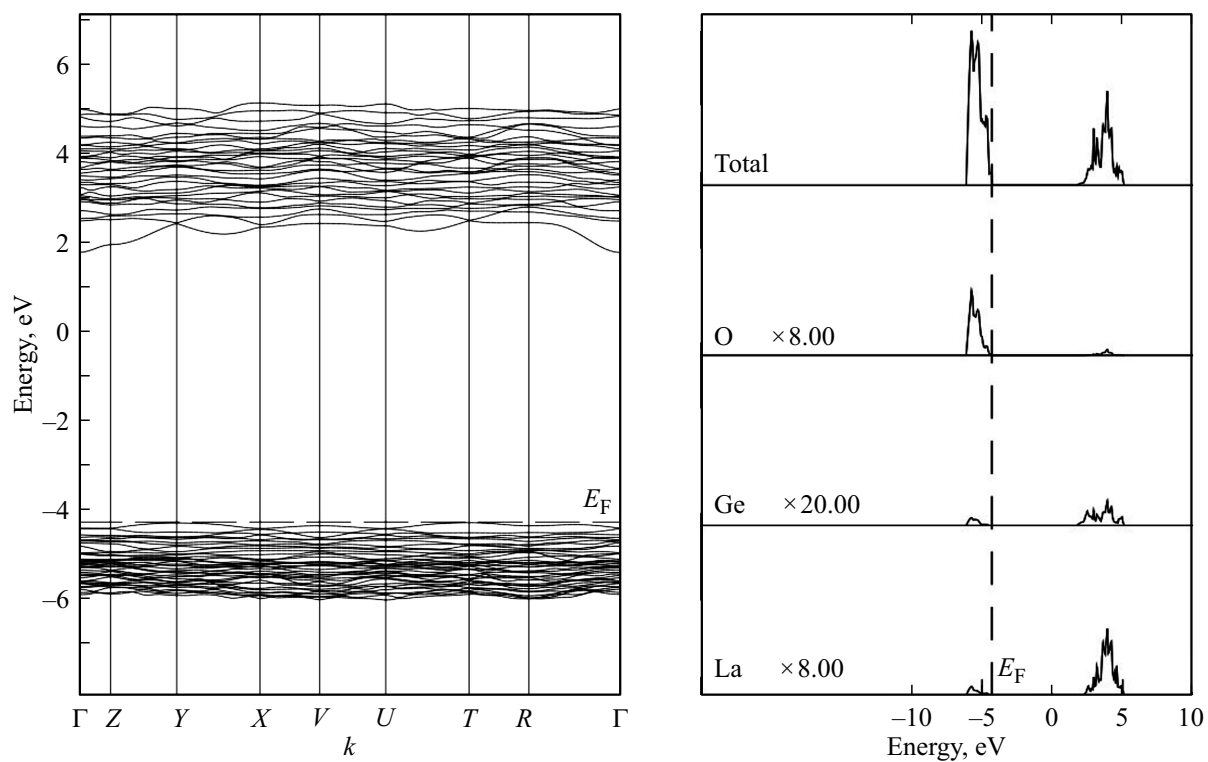


**Figure 3.** Zone structure and density of electronic states of  $\text{La}_2\text{Ge}_2\text{O}_7$  in low symmetry structure. Contributions to density of states were constructed for 1La, 9Ge, 19O ions (Table 4), which have minimum positive (maximum negative) charge among ions of this type (Table 4). I.e., contributions of ions that have the maximum number of electrons on their orbitals among ions of this type are constructed.

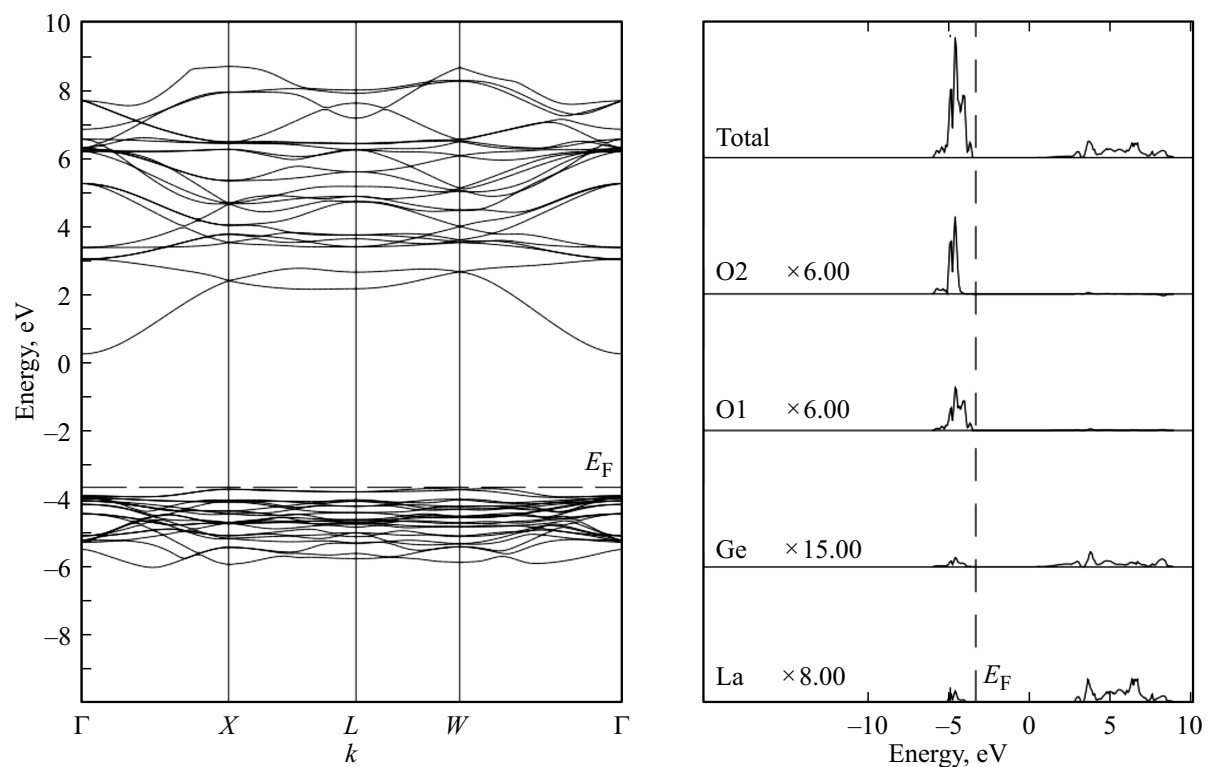


**Figure 4.** Band structure and density of electronic states of  $\text{La}_2\text{Ge}_2\text{O}_7$  in pyrochlore structure.

**Table 2.** Constant meshes and corners of elementary cell in low symmetry structure  $\text{La}_2\text{Ge}_2\text{O}_7$  (sp. gr.  $P\bar{1}$ )

	$a, \text{Å}$	$b, \text{Å}$	$c, \text{Å}$	$\alpha, \text{deg}$	$\beta, \text{deg}$	$\gamma, \text{deg}$
Calculation	7.109	7.14	12.83	93.4	90.35	90.78
Experiment [7]	$7.006 \pm 0.005$	$7.07 \pm 0.005$	$12.76 \pm 0.01$	$94.1 \pm 0.17$	$90.35 \pm 0.17$	$90.95 \pm 0.17$

**Table 3.** Ion coordinates in elementary cell  $\text{La}_2\text{Ge}_2\text{O}_7$  in shares of mesh constants. Low symmetry structure (pr. gr.  $P\bar{1}$ ),  $Z = 4$ . Calculation PBE0

Ion	$x$	$y$	$z$
1 La	0.0484	0.3253	0.1186
2 La	-0.0484	-0.3253	-0.1186
3 La	0.1223	0.0787	0.3653
4 La	-0.1223	-0.0787	-0.3653
5 La	0.3288	-0.1749	0.1089
6 La	-0.3288	0.1749	-0.1089
7 La	0.3586	0.2569	-0.3711
8 La	-0.3586	-0.2569	0.3711
9 Ge	0.1510	-0.3855	0.3886
10 Ge	-0.1510	0.3855	-0.3886
11 Ge	0.1548	0.1510	-0.1172
12 Ge	-0.1548	-0.1510	0.1172
13 Ge	0.3719	-0.2558	-0.4025
14 Ge	-0.3719	0.2558	0.4025
15 Ge	0.4920	-0.3196	-0.1715
16 Ge	-0.4920	0.3196	0.1715
17 O	0.0049	0.0024	0.1864
18 O	-0.0049	-0.0024	-0.1864
19 O	0.0050	-0.3350	0.0803
20 O	-0.0050	0.3350	-0.0803
21 O	0.0281	0.2329	-0.4337
22 O	-0.0281	-0.2329	0.4337
23 O	0.0730	0.4116	0.3200
24 O	-0.0730	-0.4116	-0.3200
25 O	0.2228	-0.0695	-0.3867
26 O	-0.2228	0.0695	0.3867
27 O	0.2355	0.0961	0.0061
28 O	-0.2355	-0.0961	-0.0061
29 O	0.2968	-0.2295	0.3212
30 O	-0.2968	0.2295	-0.3212
31 O	0.2957	-0.4348	-0.4996
32 O	-0.2957	0.4348	0.4996
33 O	0.3047	-0.2699	-0.0887
34 O	-0.3047	0.2699	0.0887
35 O	0.3488	0.2152	-0.1891
36 O	-0.3488	-0.2152	0.1891
37 O	0.3538	0.4847	0.1271
38 O	-0.3538	-0.4847	-0.1271
39 O	0.3650	0.1351	0.2130
40 O	-0.3650	-0.1351	-0.2130
41 O	0.3876	-0.4066	-0.2972
42 O	-0.3876	0.4066	0.2972
43 O	0.4166	0.1702	0.4479
44 O	-0.4166	-0.1702	-0.4479

**Table 4.** Charges of ions in low symmetry phase  $\text{La}_2\text{Ge}_2\text{O}_7$  (by Mulliken). Calculation PBE0

Ion	charge, $ e $	ion	charge, $ e $
1 La	+2.217	23 O	-1.162
2 La	+2.217	24 O	-1.162
3 La	+2.237	25 O	-1.165
4 La	+2.237	26 O	-1.165
5 La	+2.251	27 O	-1.151
6 La	+2.251	28 O	-1.151
7 La	+2.234	29 O	-1.197
8 La	+2.234	30 O	-1.197
9 Ge	+1.779	31 O	-0.962
10 Ge	+1.779	32 O	-0.962
11 Ge	+1.835	33 O	-1.170
12 Ge	+1.835	34 O	-1.170
13 Ge	+1.784	35 O	-1.213
14 Ge	+1.784	36 O	-1.213
15 Ge	+1.797	37 O	-1.152
16 Ge	+1.797	38 O	-1.152
17 O	-1.206	39 O	-1.157
18 O	-1.206	40 O	-1.157
19 O	-1.250	41 O	-0.999
20 O	-1.250	42 O	-0.999
21 O	-1.179	43 O	-1.170
22 O	-1.179	44 O	-1.170

**Table 5.** Charges on bonds in low symmetry structure  $\text{La}_2\text{Ge}_2\text{O}_7$  (by Mulliken). Calculation PBE0

Ions	Distance, $\text{Å}$	Charge on bond, $ e $
Ge9–O23	1.733	0.293
Ge9–O22	1.766	0.234
Ge9–O29	1.776	0.228
Ge9–O31	1.813	0.208
La3–O43	2.405	0.058
La3–O17	2.465	0.012
La3–O26	2.471	0.027
La3–O23	2.508	0.002
La3–O29	2.576	0.000
La3–O22	2.652	0.012
La3–O39	2.659	0.028
La3–O21	2.831	0.017

**Table 6.** Forbidden band width  $\text{La}_2\text{Ge}_2\text{O}_7$ . Calculation with DFT-functionalities of different level

Calculation	PBE, eV	B3LYP, eV	PBE0, eV
Pyrochlore structure (sp. gr. 227)	2.1	3.9	4.8
Low symmetry structure (sp. gr. 2)	3.9	6.0	6.7

**Table 7.** Frequencies and types of phonon modes in  $\Gamma$ -point  $\text{La}_2\text{Ge}_2\text{O}_7$  in pyrochlore structure. Designations in columns „IR“ and „Raman“: „A“ — active mode, „I“ — inactive

Type	IR	Raman	Frequency, $\text{cm}^{-1}$ , calculation	Ions-participants
$F_{2u}$	I	I	53	$\text{La}^S, \text{Ge}^W, \text{O1}$
$E_u$	I	I	107	$\text{La}^S, \text{Ge}, \text{O1}$
$F_{1u}$	A	I	124	$\text{La}, \text{Ge}^S, \text{O1}, \text{O}^{2S}$
$F_{1u}$	A	I	143	$\text{La}, \text{Ge}, \text{O}^{2S}$
$F_{2u}$	I	I	191	$\text{Ge}^S, \text{O1}^W$
$F_{1u}$	A	I	255	$\text{La}^W, \text{Ge}, \text{O1}^S$
$B_u$	I	I	264	$\text{Ge}^S, \text{O1}^W$
$E_u$	k	I	282	$\text{La}^W, \text{Ge}, \text{O1}^S$
$F_{1g}$	I	I	289	$\text{O1}^S$
$F_{2u}$	I	I	306	$\text{Ge}^W, \text{O1}^S$
$B_u$	I	I	331	La
$F_{1u}$	A	I	334	Ge, O1
$F_{2g}$	I	A	354	$\text{O1}^S$
$F_{1g}$	I	I	376	$\text{O1}^S$
$E_g$	I	A	385	$\text{O1}^S$
$E_u$	I	I	419	Ge, $\text{O1}^S$
$F_{1u}$	A	I	431	$\text{O1}^S$
$F_{2g}$	I	A	482	$\text{O1}^S, \text{O2}$
$F_{1u}$	A	I	499	$\text{O1}^W, \text{O}^{2S}$
$F_{1u}$	A	I	531	$\text{O1}^S, \text{O2}$
$A_g$	I	A	552	O1
$B_u$	I	I	560	O1
$F_{2u}$	I	I	578	$\text{O1}^S$
$F_{2g}$	I	A	644	$\text{O1}^W, \text{O}^{2S}$
$F_{2g}$	I	A	664	$\text{O1}^S, \text{O2}$

Note. In the last column: „S“ — strong, „W“ — weak displacement of ion in mode. Maximum displacements  $\sim 0.04 \text{ \AA}$  in La ion in low frequency mode  $F_{2u}$  ( $53 \text{ cm}^{-1}$ ), and also in oxygen ions: O1 in mode  $F_{2u}$  ( $306 \text{ cm}^{-1}$ ) and O2 in mode  $F_{1u}$  ( $499 \text{ cm}^{-1}$ ) and mode  $F_{2g}$  ( $644 \text{ cm}^{-1}$ ). If displacement value is 0.02–0.04, displacement is marked as „S“, if displacement value does not exceed 0.01, then displacement is marked as „W“, if below 0.005 — ion is not mentioned in column „ions-participants“.

The calculation predicts an indirect gap for both the low symmetry structure and pyrochlore structure. The calculation with functionalities of different levels predicts a wider gap for the low symmetry structure. The closest estimate of the forbidden gap width in compounds with ion-covalent bonding to the experiment is given by the B3LYP functionality. The calculation with non-hybrid PBE functionality gives an underestimation relative to the

experiment. The calculation with hybrid PBE0, where the fraction of XF-exchange is greater than in B3LYP, gives an overestimated value.

Near the ceiling of the valence band there are predominantly oxygen states. Near the bottom of the conduction band — lanthanum states (Figs. 3–4).

Results of calculation of phonon spectrum  $\text{La}_2\text{Ge}_2\text{O}_7$  (in  $\Gamma$ -point) are given in Tables 7–8 and in Figs. 5–6.

Values of ion displacements in phonon modes for pyrochlore structure ( $Z = 2$ ) and for low symmetry structure ( $Z = 4$ ) are shown in Figs. 5–6. In low symmetry structure in elementary cell there are 8 ions La, 8 — Ge and 28 oxygen ions. Fig. 6 gives maximum and minimum displacements of ions of one type (La, Ge, O) in phonon modes.

In low symmetry structure, La ions manifest substantial participation in modes with frequencies to  $\sim 200 \text{ cm}^{-1}$ , Ge ions — in modes with frequencies to  $\sim 450 \text{ cm}^{-1}$ ; oxygen ions participate in the entire range of frequencies. The calculation predicts a gap in phonon spectrum between  $\sim 600$  and  $\sim 670 \text{ cm}^{-1}$ . One may note strong mixing of oscillations.

Spectrum of high symmetry phase, which is not observed in the experiment, is specific for pyrochlore structure and contains much fewer frequencies. Participation of oxygen ( $\text{O1}, 48f$ ) also manifests in the entire range.

In pyrochlore structure  $\text{La}_2\text{Ge}_2\text{O}_7$  has corresponding phonon modes in  $\Gamma$ -point:  $\Gamma = A_{1g} + E_g + 2F_{1g} + 4F_{2g} + 3A_{2u} + 3E_u + 8F_{1u} + 4F_{2u}$ . Out of them one  $F_{1u}$  mode is translational,  $4F_{2u}, 3E_u, 3A_{2u}, 2F_{1g}$  — „silent“ modes, which are not active in IR or Raman. Modes  $A_{1g} + E_g + 4F_{2g}$  are active in Raman,  $7F_{1u}$  modes are active in IR.

In low symmetry structure, characterized by sp. gr.  $P\bar{1}$ ,  $\text{La}_2\text{Ge}_2\text{O}_7$  has corresponding phonon modes in  $\Gamma$ -point:  $\Gamma = 66A_g + 66A_u$ . Out of them 3 modes  $A_u$  are translational, other modes  $A_u$  are active in IR, and 66 modes  $A_g$  are active in Raman (Table 8).

In column „Dominant type of oscillation“ (Table 8) for those modes, where it is possible, a dominant type of oscillation is identified — with change of bond length („stretching“), with angle change („bending“).

The paper also calculated elastic constants. The calculation was carried out with hybrid functionality PBE0. Tensor of elastic constants (GPa) was obtained for pyrochlore structure

$$\begin{pmatrix} 312.2 & 133.8 & 133.8 & 0 & 0 & 0 \\ 133.8 & 312.3 & 133.8 & 0 & 0 & 0 \\ 133.8 & 133.8 & 312.3 & 0 & 0 & 0 \\ 0 & 0 & 0 & 106.0 & 0 & 0 \\ 0 & 0 & 0 & 0 & 106.0 & 0 \\ 0 & 0 & 0 & 0 & 0 & 106.0 \end{pmatrix}$$

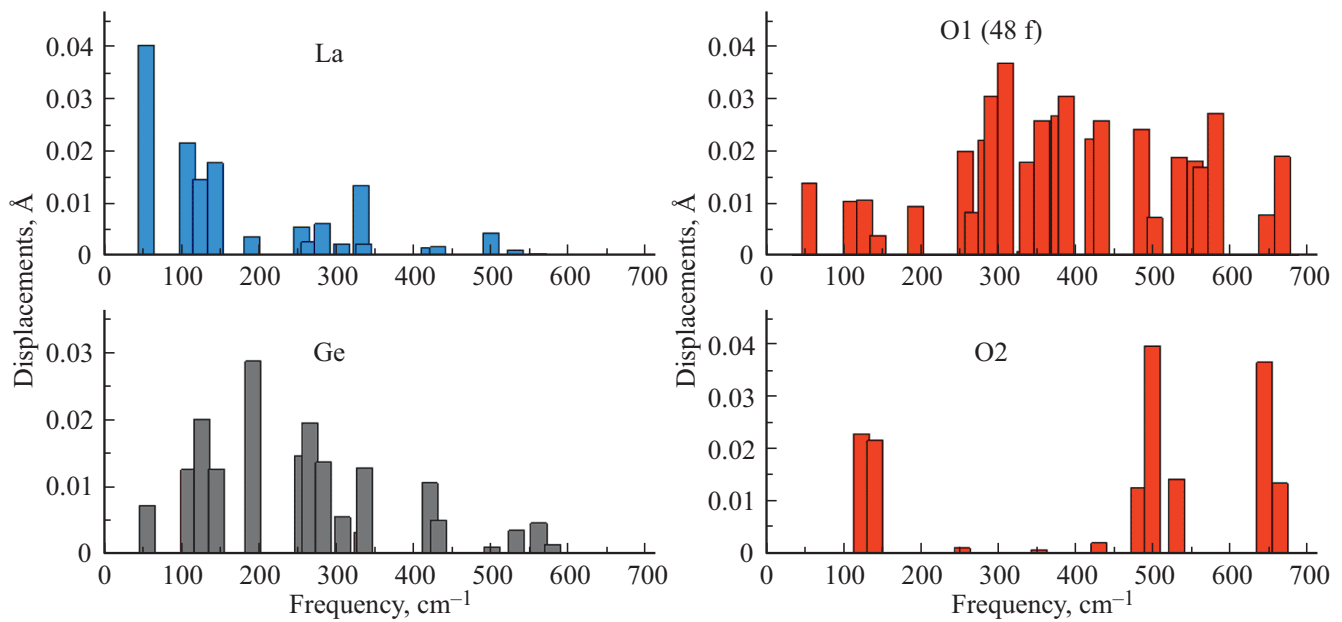


**Figure 5.** Displacements of ions in phonon modes  $\text{La}_2\text{Ge}_2\text{O}_7$ . Pyrochlore structure.

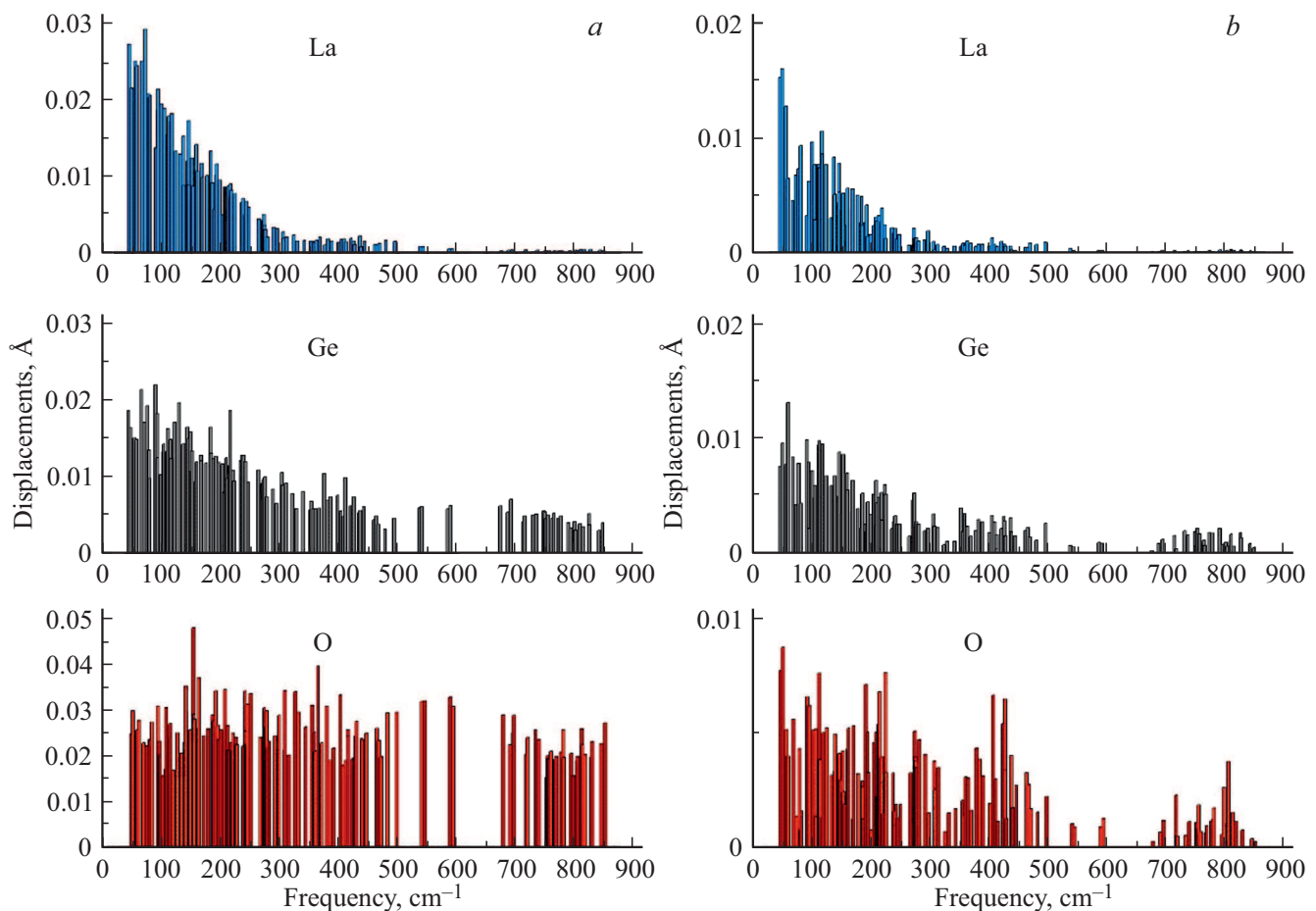


**Figure 6.** Displacements of ions in phonon modes  $\text{La}_2\text{Ge}_2\text{O}_7$ : *a*) maximum, *b*) minimum. Low symmetry structure.

**Table 8.** Frequencies and types of phonon modes in  $\Gamma$ -point  $\text{La}_2\text{Ge}_2\text{O}_7$  in low symmetry structure. Designations in columns „IR“ and „Raman“: „A“ — active mode, „I“ — inactive

Type	IR	Raman	Frequency, $\text{cm}^{-1}$ , calculation	Ions-participants	Dominant type of oscillation
$A_g$	I	A	44.9	$\text{La}^S, \text{Ge}, \text{O}^S$	Not determined
$A_g$	I	A	48.4	$\text{La}^S, \text{Ge}, \text{O}^S$	Not determined
$A_u$	A	I	54.8	$\text{La}^S, \text{Ge}, \text{O}^S$	Not determined
$A_u$	A	I	58.2	$\text{La}^S, \text{Ge}, \text{O}^S$	Not determined
$A_g$	I	A	66.4	$\text{La}^S, \text{Ge}^S, \text{O}^S$	Not determined
$A_g$	I	A	71.7	$\text{La}^S, \text{Ge}, \text{O}^S$	Not determined
$A_u$	A	I	76.6	$\text{La}^S, \text{Ge}, \text{O}^S$	Not determined
$A_g$	I	A	79.6	$\text{La}^S, \text{Ge}, \text{O}^S$	Not determined
$A_u$	A	I	80.3	$\text{La}^S, \text{Ge}^W, \text{O}^S$	Not determined
$A_g$	I	A	90.1	$\text{La}, \text{Ge}^S, \text{O}^S$	Not determined
$A_u$	A	I	93.4	$\text{La}, \text{Ge}, \text{O}^S$	Not determined
$A_g$	I	A	93.7	$\text{La}^S, \text{Ge}, \text{O}$	Not determined
$A_g$	I	A	99.4	$\text{La}, \text{Ge}, \text{O}$	Not determined
$A_g$	I	A	103.7	$\text{La}, \text{Ge}, \text{O}$	bending (O–La–O)
$A_u$	A	I	104.2	$\text{La}, \text{Ge}, \text{O}^S$	bending (O–La–O)
$A_u$	A	I	110.4	$\text{La}, \text{Ge}, \text{O}^S$	bending (O–La–O)
$A_g$	I	A	111.4	$\text{La}, \text{Ge}, \text{O}^S$	bending (O–La–O)
$A_u$	A	I	115.6	$\text{La}, \text{Ge}, \text{O}$	bending (O–La–O)
$A_g$	I	A	116.6	$\text{La}, \text{Ge}, \text{O}$	bending (O–La–O)
$A_u$	A	I	123.3	$\text{La}, \text{Ge}, \text{O}^S$	bending (O–La–O) bending (La–O–Ge)
$A_g$	I	A	131.0	$\text{La}, \text{Ge}, \text{O}^S$	bending (O–La–O)
$A_g$	I	A	136.2	$\text{La}, \text{Ge}, \text{O}^S$	bending (O–La–O)
$A_u$	A	I	137.8	$\text{La}^W, \text{Ge}, \text{O}^S$	bending (O–La–O)
$A_g$	I	A	144.4	$\text{La}, \text{Ge}, \text{O}^S$	bending (O–La–O) other (O–Ge–O)
$A_u$	A	I	145.3	$\text{La}, \text{Ge}^W, \text{O}^S$	bending (O–La–O)
$A_u$	A	I	145.7	$\text{La}^W, \text{Ge}, \text{O}^S$	bending (O–La–O)
$A_g$	I	A	150.2	$\text{La}^W, \text{Ge}, \text{O}^S$	bending (O–La–O)
$A_u$	A	I	151.5	$\text{La}, \text{Ge}, \text{O}^S$	bending (O–La–O)
$A_g$	I	A	152.5	$\text{La}^W, \text{Ge}, \text{O}^S$	bending (O–La–O) bending (O–Ge–O)
$A_u$	A	I	158.6	$\text{La}, \text{Ge}^W, \text{O}^S$	bending (O–La–O)
$A_g$	I	A	159.8	$\text{La}, \text{Ge}, \text{O}^S$	bending (O–La–O)
$A_g$	I	A	167.5	$\text{La}, \text{Ge}, \text{O}^S$	bending (O–La–O)

Table 8 (continued).

Type	IR	Raman	Frequency, cm <sup>-1</sup> , calculation	Ions-participants	Dominant type of oscillation
A <sub>u</sub>	A	I	168.1	La <sup>W</sup> , Ge, O <sup>S</sup>	bending (O–La–O) other (O–Ge–O)
A <sub>g</sub>	I	A	176.2	La, Ge, O <sup>S</sup>	bending (O–La–O) bending (O–Ge–O)
A <sub>u</sub>	A	I	183.2	La, Ge, O <sup>S</sup>	bending (O–La–O)
A <sub>u</sub>	A	I	183.6	La <sup>W</sup> , Ge, O <sup>S</sup>	bending (O–La–O)
A <sub>g</sub>	I	A	184.8	La <sup>W</sup> , Ge, O <sup>S</sup>	bending (O–La–O)
A <sub>u</sub>	A	I	188.7	La <sup>W</sup> , Ge, O <sup>S</sup>	bending (O–La–O)
A <sub>u</sub>	A	I	192.1	La, Ge <sup>W</sup> , O <sup>S</sup>	bending (O–La–O) other (O–Ge–O)
A <sub>g</sub>	I	A	193.4	La, Ge, O <sup>S</sup>	stretching (O–La) bending (O–La–O)
A <sub>g</sub>	I	A	198.0	La <sup>W</sup> , Ge, O <sup>S</sup>	bending (O–La–O)
A <sub>g</sub>	I	A	203.7	Ge, O <sup>S</sup>	bending (O–Ge–O)
A <sub>u</sub>	A	I	207.1	La <sup>W</sup> , Ge <sup>W</sup> , O <sup>S</sup>	bending (O–La–O)
A <sub>u</sub>	A	I	208.0	La <sup>W</sup> , Ge <sup>W</sup> , O <sup>S</sup>	bending (O–La–O)
A <sub>g</sub>	I	A	210.2	La <sup>W</sup> , Ge, O <sup>S</sup>	bending (O–La–O) stretching (O–La)
A <sub>g</sub>	I	A	212.3	La <sup>W</sup> , Ge <sup>W</sup> , O <sup>S</sup>	bending (O–La–O) bending (O–Ge–O) stretching (O–La)
A <sub>u</sub>	A	I	215.8	La <sup>W</sup> , Ge, O <sup>S</sup>	stretching (O–La) bending (O–La–O) bending (O–Ge–O)
A <sub>g</sub>	I	A	216.4	La <sup>W</sup> , Ge, O <sup>S</sup>	stretching (O–La) bending (O–La–O)
A <sub>u</sub>	A	I	217.7	La <sup>W</sup> , Ge, O <sup>S</sup>	bending (O–La–O) stretching (O–La)
A <sub>g</sub>	I	A	222.7	Ge, O <sup>S</sup>	bending (O–La–O) bending (O–Ge–O)
A <sub>u</sub>	A	I	224.1	La <sup>W</sup> , Ge <sup>W</sup> , O <sup>S</sup>	bending (O–Ge–O)
A <sub>u</sub>	A	I	234.9	La <sup>W</sup> , Ge, O <sup>S</sup>	bending (O–La–O) bending (O–Ge–O)
A <sub>g</sub>	I	A	237.9	La <sup>W</sup> , Ge <sup>W</sup> , O <sup>S</sup>	bending (O–La–O) other (O–Ge–O)
A <sub>u</sub>	A	I	238.4	La <sup>W</sup> , Ge, O <sup>S</sup>	other (O–Ge–O)
A <sub>g</sub>	I	A	240.2	Ge, O <sup>S</sup>	stretching (O–La) bending (O–Ge–O)
A <sub>g</sub>	I	A	242.8	La <sup>W</sup> , Ge, O <sup>S</sup>	other (O–La–O) bending (O–La–O) bending (O–Ge–O)

**Table 8** (*continued*).

Type	IR	Raman	Frequency, $\text{cm}^{-1}$ , calculation	Ions-participants	Dominant type of oscillation
$A_u$	A	I	247.7	$\text{La}^W, \text{Ge}^W, \text{O}^S$	bending (O–Ge–O) other (O–La–O)
$A_u$	A	I	264.4	$\text{Ge}, \text{O}^S$	bending (O–La–O) other (O–Ge–O)
$A_u$ 1053gg	A	I	270.3	$\text{Ge}^W, \text{O}^S$	bending (O–La–O) other (O–Ge–O)
$A_g$	I	A	271.7	$\text{Ge}^W, \text{O}^S$	stretching (O–La) bending (O–La–O)
$A_g$	I	A	272.7	$\text{La}^W, \text{Ge}^W, \text{O}$	stretching (O–La) bending (O–Ge–O)
$A_u$	A	I	274.2	$\text{Ge}^W, \text{O}^S$	other (O–Ge–O)
$A_u$	A	I	275.8	$\text{Ge}^W, \text{O}^S$	bending (O–Ge–O)
$A_g$	I	A	279.4	$\text{Ge}^W, \text{O}^S$	bending (O–Ge–O)
$A_g$	I	A	289.4	$\text{Ge}^W, \text{O}^S$	stretching (O–La) bending (O–La–O) bending (O–Ge–O)
$A_g$	I	A	295.9	$\text{Ge}^W, \text{O}^S$	bending (O–Ge–O)
$A_u$	A	I	305.1	$\text{Ge}, \text{O}^S$	bending (O–Ge–O)
$A_u$	A	I	306.1	$\text{Ge}^W, \text{O}^S$	bending (La–O–Ge) bending (Ge–O–La)
$A_g$	I	A	312.0	$\text{Ge}^W, \text{O}^S$	bending (O–Ge–O)
$A_u$	A	I	323.1	$\text{Ge}^W, \text{O}^S$	bending (O–La–O) other (O–Ge–O)
$A_g$	I	A	329.1	$\text{Ge}^W, \text{O}^S$	bending (O–La–O) bending (O–Ge–O)
$A_u$	A	I	340.9	$\text{Ge}^W, \text{O}^S$	bending (O–Ge–O)
$A_g$	I	A	352.1	$\text{Ge}^W, \text{O}^S$	bending (O–Ge–La)
$A_g$	I	A	355.1	$\text{Ge}^W, \text{O}^S$	stretching (O–La) bending (La–O–La) bending (Ge–O–La)
$A_u$	A	I	357.8	$\text{Ge}^W, \text{O}^S$	bending (O–Ge–O)
$A_u$	A	I	361.9	$\text{Ge}^W, \text{O}^S$	stretching (O–La) bending (La–O–Ge) bending (Ge–O–La)
$A_g$	I	A	368.0	$\text{Ge}^W, \text{O}^S$	bending (O–La–O)
$A_u$	A	I	376.6	$\text{Ge}, \text{O}^S$	bending (Ge–O–La)
$A_u$	A	I	381.7	$\text{Ge}^W, \text{O}$	bending (Ge–O–La)
$A_g$	I	A	388.0	$\text{Ge}^W, \text{O}^S$	bending (O–Ge–O) bending (Ge–O–La)
$A_u$	A	I	399.5	$\text{Ge}^W, \text{O}^S$	bending (O–Ge–O)
$A_g$	I	A	404.9	$\text{Ge}^W, \text{O}$	bending (O–Ge–O)
$A_u$	A	I	408.4	O	bending (O–Ge–O)

Table 8 (continued).

Type	IR	Raman	Frequency, cm <sup>-1</sup> , calculation	Ions-participants	Dominant type of oscillation
A <sub>u</sub>	A	I	412.5	Ge <sup>W</sup> , O <sup>S</sup>	bending (O–Ge–O) bending (Ge–O–La)
A <sub>g</sub>	I	A	412.6	Ge <sup>W</sup> , O <sup>S</sup>	bending (O–Ge–O) bending (Ge–O–La)
A <sub>g</sub>	I	A	420.4	Ge <sup>W</sup> , O	bending (O–Ge–O)
A <sub>g</sub>	I	A	424.5	Ge <sup>W</sup> , O	stretching (O–La) bending (O–Ge–O)
A <sub>g</sub>	I	A	425.0	O <sup>S</sup>	stretching (O–La) bending (O–Ge–O)
A <sub>u</sub>	A	I	427.0	Ge <sup>W</sup> , O <sup>S</sup>	bending (O–Ge–O) bending (Ge–O–La)
A <sub>u</sub>	A	I	435.6	Ge <sup>W</sup> , O <sup>S</sup>	stretching (La–O–Ge) bending (Ge–O–La)
A <sub>u</sub>	A	I	437.3	Ge <sup>W</sup> , O <sup>S</sup>	bending (Ge–O–La)
A <sub>g</sub>	I	A	443.8	Ge <sup>W</sup> , O <sup>S</sup>	bending (Ge–O–La)
A <sub>g</sub>	I	A	461.6	O <sup>S</sup>	stretching (O–La) bending (Ge–O–La)
A <sub>u</sub>	A	I	465.3	O <sup>S</sup>	bending (Ge–O–La)
A <sub>g</sub>	I	A	469.2	O	stretching (O–La) bending (O–Ge–O)
A <sub>g</sub>	I	A	479.9	O <sup>S</sup>	stretching (La–O–La) stretching (O–La–O) bending (O–Ge–O)
A <sub>u</sub>	A	I	495.1	O <sup>S</sup>	stretching (La–O–La) bending (Ge–O–La)
A <sub>u</sub>	A	I	537.9	Ge <sup>W</sup> , O <sup>S</sup>	bending (O–Ge–O) bending (Ge–O–Ge)
A <sub>g</sub>	I	A	542.7	Ge <sup>W</sup> , O <sup>S</sup>	bending (Ge–O–Ge)
A <sub>u</sub>	A	I	586.0	Ge <sup>W</sup> , O <sup>S</sup>	bending (Ge–O–Ge)
A <sub>g</sub>	I	A	591.3	Ge <sup>W</sup> , O <sup>S</sup>	bending (O–Ge–O) bending (Ge–O–Ge)
A <sub>u</sub>	A	I	675.7	Ge <sup>W</sup> , O <sup>S</sup>	stretching (O–Ge)
A <sub>g</sub>	I	A	687.4	Ge <sup>W</sup> , O <sup>S</sup>	stretching (O–Ge)
A <sub>g</sub>	I	A	693.1	Ge <sup>W</sup> , O <sup>S</sup>	stretching (O–Ge)
A <sub>u</sub>	A	I	693.4	Ge <sup>W</sup> , O <sup>S</sup>	stretching (O–Ge)
A <sub>u</sub>	A	I	714.3	O <sup>S</sup>	stretching (O–Ge)
A <sub>g</sub>	I	A	716.9	O <sup>S</sup>	stretching (O–Ge)
A <sub>u</sub>	A	I	730.7	O <sup>S</sup>	stretching (O–Ge)
A <sub>g</sub>	I	A	736.4	Ge <sup>W</sup> , O <sup>S</sup>	stretching (O–Ge)
A <sub>g</sub>	I	A	749.2	Ge <sup>W</sup> , O	stretching (O–Ge)
A <sub>u</sub>	A	I	751.1	Ge <sup>W</sup> , O	stretching (O–Ge)

Table 8 (continued).

Type	IR	Raman	Frequency, $\text{cm}^{-1}$ , calculation	Ions-participants	Dominant type of oscillation
$A_u$	A	I	753.0	O	stretching (O–Ge)
$A_g$	I	A	756.8	$\text{O}^S$	stretching (O–Ge)
$A_g$	I	A	763.9	O	stretching (O–Ge)
$A_u$	A	I	766.0	$\text{Ge}^W, \text{O}$	stretching (O–Ge)
$A_g$	I	A	773.6	$\text{O}^S$	stretching (O–Ge)
$A_u$	A	I	777.8	$\text{O}^S$	stretching (O–Ge)
$A_g$	I	A	778.3	O	stretching (O–Ge)
$A_g$	I	A	791.1	$\text{O}^S$	stretching (O–Ge)
$A_u$	A	I	795.0	O	stretching (Ge–O–Ge)
$A_u$	A	I	801.1	O	stretching (Ge–O) bending (La–O–Ge)
$A_g$	I	A	802.8	O	bending (O–La–O) stretching (O–Ge) stretching (O–La–O)
$A_g$	I	A	809.2	$\text{O}^S$	bending (La–O–Ge) stretching (O–Ge)
$A_u$	A	I	810.0	$\text{O}^S$	stretching (O–Ge)
$A_u$	A	I	815.1	$\text{O}^S$	stretching (O–Ge)
$A_u$	A	I	825.8	$\text{Ge}^W, \text{O}$	stretching (O–Ge)
$A_g$	I	A	826.7	$\text{O}^S$	stretching (O–Ge) stretching (Ge–O–Ge) bending (La–O–Ge)
$A_u$	A	I	842.4	$\text{O}^S$	stretching (O–Ge) bending (La–O–Ge)
$A_g$	I	A	848.8	$\text{O}^S$	stretching (O–Ge)

Note. Maximum displacements  $\sim 0.03 \text{ \AA}$  in ion La in low frequency mode  $A_g$  ( $71.7 \text{ cm}^{-1}$ ), and also in oxygen ion  $0.05 \text{ \AA}$  in mode  $A_g$  ( $150.2 \text{ cm}^{-1}$ ). If displacement value is  $0.02\text{--}0.04$ , displacement is marked as „ $S^*$ “; if displacement value does not exceed  $0.01$ , then displacement is marked as „ $W^*$ “, if below  $0.005$  — ion is not mentioned in column „ions-participants“.

and for low symmetry structure

$$\begin{pmatrix} 180.4 & 69.4 & 84.3 & -0.2 & 15.7 & -2.3 \\ 69.4 & 204.9 & 69.4 & 0.6 & 6.1 & 0.9 \\ 84.3 & 69.4 & 163.6 & 15.6 & 1.2 & -1.4 \\ -0.2 & 0.6 & 15.6 & 22.6 & 9.2 & 4.2 \\ 15.7 & 6.1 & 1.2 & 9.2 & 37.1 & -1.0 \\ -2.30 & 0.9 & -1.4 & 4.2 & -1.0 & 34.0 \end{pmatrix}.$$

For cubic structure — pyrochlore — conditions of mechanical stability are met (Born criteria):

$$C_{11} > |C_{12}|,$$

$$C_{11} > 0,$$

$$C_{44} > 0,$$

$$(C_{11} + 2C_{12}) > 0.$$

Thus, calculations predict for  $\text{La}_2\text{Ge}_2\text{O}_7$  a stable pyrochlore structure, which is less advantageous by energy compared to low symmetry structure. Conditions of mechanical stability for low symmetry monoclinic structure [16] are also met (Table 9).

Results of elastic moduli calculation are given in Table 10.

In Table 10 gives elastic moduli, Poisson ratio, universal anisotropy index  $A^U$  for  $\text{La}_2\text{Ge}_2\text{O}_7$ . Ratio of volume modulus to shear modulus  $G/B$ , value of Poisson ratio are illustrative of the fact that  $\text{La}_2\text{Ge}_2\text{O}_7$  in low symmetry

**Table 9.** Conditions of mechanical stability for monoclinic structure [16] La<sub>2</sub>Ge<sub>2</sub>O<sub>7</sub>

Condition	Value of left part
$C_{11} > 0$	180
$C_{22} > 0$	205
$C_{33} > 0$	164
$C_{44} > 0$	23
$C_{55} > 0$	37
$C_{66} > 0$	34
$[C_{11} + C_{22} + C_{33} + 2(C_{12} + C_{13} + C_{23})] > 0$	986
$(C_{33}C_{55} - C_{35}^2) > 0$	6071
$(C_{44}C_{66} - C_{46}^2) > 0$	763
$(C_{22} + C_{33} - 2C_{23}^2) > 0$	239
$(C_{22}(C_{33}C_{55} - C_{35}^2) + 2C_{23}C_{25}C_{35} - C_{23}^2C_{55} - C_{25}^2C_{33}) > 0$	1082101
$\{2[C_{15}C_{25}(C_{33}C_{12} - C_{13}C_{23}) + C_{15}C_{35}(C_{22}C_{13} - C_{12}C_{23}) + C_{25}C_{35}(C_{11}C_{23} - C_{12}C_{13})] - [C_{15}^2(C_{22}C_{33} - C_{23}^2) + C_{25}^2(C_{11}C_{33} - C_{13}^2) + C_{35}^2(C_{11}C_{22} - C_{12}^2)] + C_{22}g\} > 0,$ where $g = C_{11}C_{22}C_{33} - C_{11}C_{23}^2 - C_{22}C_{13}^2 - C_{33}C_{12}^2 + 2C_{12}C_{13}C_{23}$ ( $g = 3801225.9$ )	788680879

**Table 10.** Volume modulus, shear modulus, etc. La<sub>2</sub>Ge<sub>2</sub>O<sub>7</sub>, GPa. (Calculation PBE0)

Structure	Arrangement of calculation	Volume modulus	Modulus Young	Modulus shear	Coefficient Poisson	$G_H/B_H$	$A^U$
Pyrochlore	Voigt	193.3	254.2	99.2	0.281	0.51	0.036
	Reuss	193.3	252.7	98.5	0.282		
	Hill	193.3	253.4	98.9	0.282		
Low symmetry	Voigt	109.6	109.0	40.8	0.334	0.33	1.715
	Reuss	106.8	83.6	30.5	0.370		
	Hill	108.2	96.4	35.7	0.351		

structure relates to plastic materials, and in pyrochlore structure it is close to brittle ones [17].

Calculation of elastic moduli in Voigt and Reuss approximations (Table 10) provides close results for pyrochlore structure, while for low symmetry structure these results differ significantly. Accordingly, the value of universal anisotropy index  $A^U$  [18] (1) for low symmetry structure differs significantly from zero

$$A^U = 5 \frac{G_V}{G_R} + \frac{B_V}{B_R} - 6. \tag{1}$$

In equation (1)  $G_V$ ,  $G_R$ ,  $B_V$ ,  $B_R$  — shear modulus and volume compression modulus, calculated in Voigt and Reuss approximations. The stronger anisotropy of elastic properties, the more is the difference of index  $A^U$  from zero.

**Table 11.** Vickers hardness, GPa

Structure pyrochlore	Low symmetry structure
11.1	3.3

Anisotropy of elastic properties in low symmetry structure is illustrated in Fig. 7.

To assess hardness of perchlorates, paper [17] successfully used formula expressing Vickers hardness  $H_V$  through volume elastic modulus and shear modulus. This empirical equation was proposed in paper [19], based on the fact that for polycrystalline samples there are correlations between Vickers hardness and ratio of shear modulus and volume

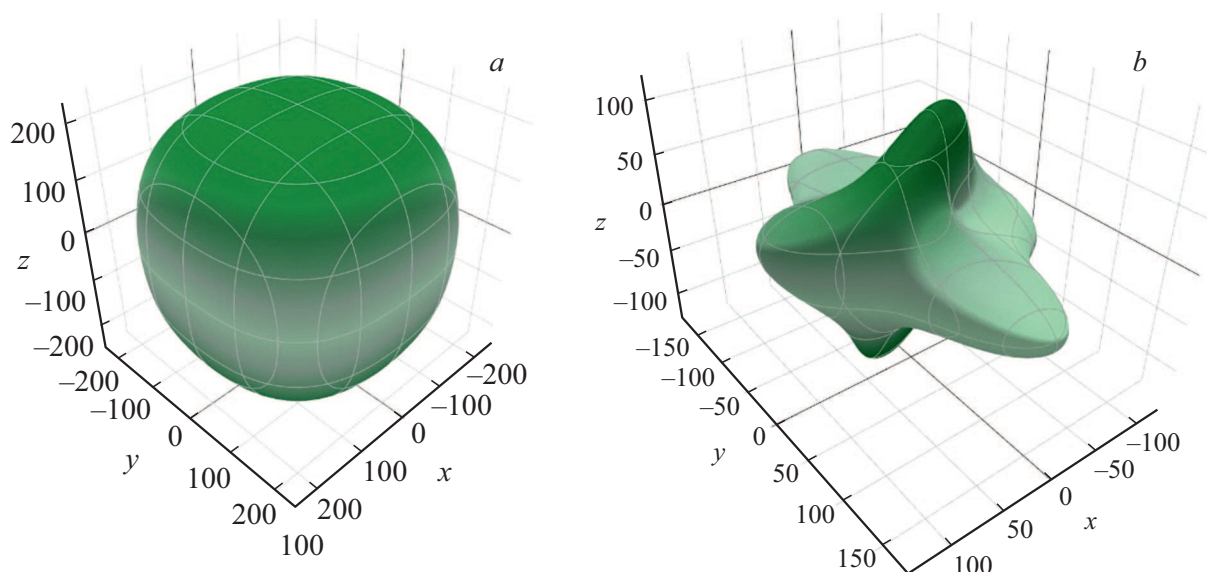


**Figure 7.** Dependence of Young modulus (in GPa) on direction in a crystal for  $\text{La}_2\text{Ge}_2\text{O}_7$ : *a*) pyrochlore structure, *b*) low symmetry structure.

compression  $G/B$ . It looks like

$$H_V = C \left( \frac{G}{B} \right)^m G^n. \quad (2)$$

In equation (2)  $H_V$  — Vickers hardness,  $G$  — shear modulus,  $B$  — volume compression modulus,  $C$  — proportion ratio. In paper [19] parameters of this equation were determined, which made it possible to describe hardness of multiple compounds, over forty, with various type of chemical bond, ion and covalent

$$H_V = 0.92 \left( \frac{G}{B} \right)^{1.137} G^{0.708}. \quad (3)$$

Equation (3) uses shear modulus  $G$  and volume compression modulus  $B$ , calculated in Hill approximation. Calculation of hardness (3) predicts hardness of  $\text{La}_2\text{Ge}_2\text{O}_7$  in low symmetry structure is lower than in pyrochlore structure (Table 11).

## 4. Conclusion

As a result of calculations *ab initio*, a complex of properties of  $\text{La}_2\text{Ge}_2\text{O}_7$  low symmetry structure was studied. It was demonstrated that low symmetry structure  $\text{La}_2\text{Ge}_2\text{O}_7$  (sp. gr.  $P\bar{1}$ ) is more energetically advantageous than pyrochlore structure, which corresponds to available experimental data from X-ray diffraction analysis. Phonon spectrum and elastic properties of  $\text{La}_2\text{Ge}_2\text{O}_7$  were studied for the first time. Calculations predict a gap in phonon spectrum of low symmetry structure between  $\sim 600$  and  $\sim 670 \text{ cm}^{-1}$ . Frequencies and types of fundamental oscillations were determined. It was demonstrated that in low

symmetry structure, La ions manifest substantial participation in modes with frequencies to  $\sim 200 \text{ cm}^{-1}$ , Ge ions — in modes with frequencies to  $\sim 450 \text{ cm}^{-1}$ , oxygen ions participate in the entire range of frequencies. Calculations predict that  $\text{La}_2\text{Ge}_2\text{O}_7$  in low symmetry structure relates to plastic materials. According to calculations, Vickers hardness of  $\text{La}_2\text{Ge}_2\text{O}_7$  in low symmetry structure is considerably lower than in pyrochlore structure. Calculations of band structure predict that forbidden gap width in low symmetry structure is considerably higher than in pyrochlore structure (6.0 and 3.9 eV accordingly — calculation with B3LYP functionality).

## Funding

This study was financially supported by the Ministry of Education and Science of the Russian Federation (project № FEUZ-2020-0054).

## Conflict of interest

The authors declare that they have no conflict of interest.

## References

- [1] G. Bocquillon, C. Chateau, J. Loriers. In: Proceed. 14<sup>th</sup> Rare Earth Res. Conf. / Eds G.J. Mc Carthy, J.J. Rhyne, H.B. Silber. Plenum Publishing Corporation, N. Y. (1980).
- [2] E. Morosan, J.A. Fleitman, Q. Huang, J.W. Lynn, Y. Chen, X. Ke, M.L. Dahlberg, P. Schiffer, C.R. Craley, R.J. Cava. *Phys. Rev. B* **77**, 22, 224423 (2008).
- [3] Q. Li, S. Zhang, W. Lin, W. Li, Y. Li, Z. Mu, F. Wu. *Spectrochim. Acta A* **228**, 117755 (2020).
- [4] K. Stadnicka, A.M. Glazer, M. Koralewski, B.M. Wanklyn. *J. Phys. Condens. Matter* **2**, 22, 4795 (1990).

- [5] I. Yaeger, R. Shuker, B.M. Wanklyn. *Phys. Status Solidi B* **104**, 2, 621 (1981).
- [6] L.N. Demyanets, A.N. Lobachev, G.A. Emelchenko. *Germanaty redkozemelnykh elementov*. Nauka, M. (1980). 152 p. (in Russian).
- [7] Yu.I. Smolin, Yu.F. Shepelev, T.V. Upatova. *Dokl. AN SSSR* **187**, 2, 322 (1969). (in Russian).
- [8] J. Yang, M. Shahid, M. Zhao, J. Feng, C. Wan, W. Pan. *J. Alloys. Compd.* **663**, 834 (2016).
- [9] Materials Project. Electronic source. Available at: <https://materialsproject.org/materials/mp-621945/#>
- [10] Materials Project. Electronic source. Available at: <https://materialsproject.org/materials/mp-21532/#>
- [11] J.P. Perdew, M. Ernzerhof, K. Burke. *J. Chem. Phys.* **105**, 22, 9982 (1996).
- [12] A.V. Arbuznikov. *Zhurn. strukturn. khimii* **48**, 5 (2007). (in Russian).
- [13] F. Corá. *Mol. Phys.* **103**, 18, 2483 (2005).
- [14] G. Sophia, P. Baranek, C. Sarrazin, M. Rerat, R. Dovesi. Systematic influence of atomic substitution on the phase diagram of ABO<sub>3</sub> ferroelectric perovskites. Unpublished work (2013). Electronic source. Available at: [http://www.crystal.unito.it/Basis\\_Sets/tin.html](http://www.crystal.unito.it/Basis_Sets/tin.html)
- [15] Energy-consistent Pseudopotentials of the Stuttgart/Cologne Group. Electronic source. Available at: <http://www.tc.uni-koeln.de/PP/clickpse.en.html>
- [16] Z.J. Wu, E.J. Zhao, H.P. Xiang, X.F. Hao, X.J. Liu, J. Meng. *Phys. Rev. B* **76**, 5, 054115 (2007).
- [17] D.V. Korabelnikov, Yu.N. Zhuravlev. *FTT* **58**, 6, 1129 (2016). (in Russian)
- [18] S.I. Ranganathan, M. Ostoja-Starzewski. *Phys. Rev. Lett.* **101**, 5, 055504 (2008).
- [19] X.Q. Chen, H.Y. Niu, D.Z. Li, Y.Y. Li. *Intermetallics* **19**, 9, 1275 (2011).
- [20] Y. Tian, B. Xu, Z. Zhao. *Int. J. Refract. Met. Hard Mater.* **33**, 93 (2012).